Rotationally Resolved Electronic Spectra of 2- and 3-Methylanisole in the Gas Phase: A Study of Methyl Group Internal Rotation†

Leonardo Alvarez-Valtierra, John T. Yi, and David W. Pratt*

Department of Chemistry, University of Pittsburgh, Pittsburgh, Pennsylvania 15260

Received: April 3, 2006; In Final Form: May 23, 2006

Rotationally resolved fluorescence excitation spectra of several torsional bands in the $S_1 \leftarrow S_0$ electronic spectra of 2-methylanisole (2MA) and 3-methylanisole (3MA) have been recorded in the collision-free environment of a molecular beam. Some of the bands can be fit with rigid rotor Hamiltonians; others exhibit perturbations produced by the coupling between the internal rotation of the methyl group and the overall rotation of the entire molecule. Analyses of these data show that 2MA and 3MA both have planar heavy-atom structures; 2MA has *trans*-disposed methyl and methoxy groups, whereas 3MA has both *cis*- and *trans*-disposed substituents. The preferred orientations (staggered or eclipsed) in two of the conformers and the internal rotation barriers of the methyl groups in all three conformers change when they are excited by light. Additionally, the values of the barriers opposing their motion depend on the relative positions of the substituent groups, in both electronic states. In contrast, no torsional motions of the attached methoxy groups were detected. Possible reasons for these behaviors are discussed.

1. Introduction

The phenomenon of internal rotation has been a subject of considerable interest to both chemists and physicists for many years. In 1936, on the basis of thermodynamic evidence, it was concluded that the relative rotation of the two methyl groups in ethane was not entirely free but was shown to be restricted by a potential barrier.[1] Subsequently, following pioneering studies of the origins of such barriers,[2] much research has been performed on many molecules containing methyl groups.[3] Two molecules of special interest to us are toluene (methylbenzene) and anisole (methoxybenzene). Recent studies of these two species have revealed that the methyl group internal rotation in toluene is relatively free,[4] whereas that in anisole is relatively rigid.[5] In the present study, we focus on molecules containing both of these functional groups, 2-methylanisole (2MA) and 3-methylanisole (3MA); see below. Our interest is in learning about how the torsional degrees of freedom in these two molecules might be influenced by each other.

Previous investigations of 2MA and 3MA have included studies of their TOF-MS,[6] LIF,[7,8] PFI-ZEKE,[9] hole-burning,[7,8] and dispersed fluorescence[6,7] spectra. These studies have revealed that both molecules exhibit significant low frequency Franck−Condon activity in their $S_1 \leftarrow S_0$ electronic spectra, evidencing some kind of conformational change produced by the absorption of light, presumably involving one or more torsional modes. Additionally, others[10,11] have described *ab initio* calculations of the ground-state methyl group internal rotation potentials for several toluene derivatives. Computed barriers at the Hartree−Fock (HF) level using medium sized basis sets agree reasonably with experimental results, for several *ortho*-substituted toluenes. But the agreement is poor for *meta*- and *para*-substituted compounds, even in their ground states. Capturing the dependence of these barriers on the electronic state of the molecule is an even more challenging task.

More data are needed to rectify this situation. In what follows, we describe both the low and high resolution $S_1 \leftarrow S_0$ fluorescence excitation spectra of 2MA and 3MA, as isolated species in the gas phase. We derive from these data information about the structures of the molecules, the preferred orientations of their substituent groups, and the barriers to methyl group internal rotation in both electronic states. The results show that the magnitude and signs of these barriers are a sensitive function of the relative position of the substituent groups and the electronic state of the molecules to which they are attached.

2. Experimental Section

2MA and 3MA were purchased from Aldrich and used without further purification. Dry argon and helium were used in all experiments as inert carrier gases.

In the vibrationally resolved experiments, samples were seeded into 60 psi of helium gas and expanded into a vacuum chamber (10^{-5} Torr) through a 1 mm diameter orifice pulsed valve (General Valve Series 9) operating at 10 Hz. Two centimeters downstream of the valve, the free jet was excited with the second harmonic of a Quanta Ray Nd^{3+}:YAG (Model DCR-1A) pumped dye laser (Model PDL-1). The dye (Rhodamine 575) laser output was frequency doubled with an external β-barium borate (BBO) crystal providing a spectral resolution of $\sim$0.6 cm^{-1} in the UV. From the point of intersection between the jet and the laser beam, the molecules were excited and the fluorescence was collected with a photomultiplier tube (PMT). Finally, the collected data were processed by a boxcar integrator (Stanford Research Systems) and recorded with Quick Data Acquisition software (version 1.0.5).

Rotationally resolved electronic experiments were performed using a molecular beam laser spectrometer, described in detail elsewhere.[12] Briefly, the molecular beam was formed by expansion of the vaporized sample (either 2MA or 3MA) seeded in argon carrier gas (−18 psi) through a heated ($\sim$313 K) 240 μm quartz nozzle into a differentially pumped vacuum system.

† Part of the special issue "Charles B. Harris Festschrift".

* To whom correspondence should be addressed. E-mail: pratt@pitt.edu.

10.1021/jp062050h CCC: $33.50
Published on Web 07/19/2006

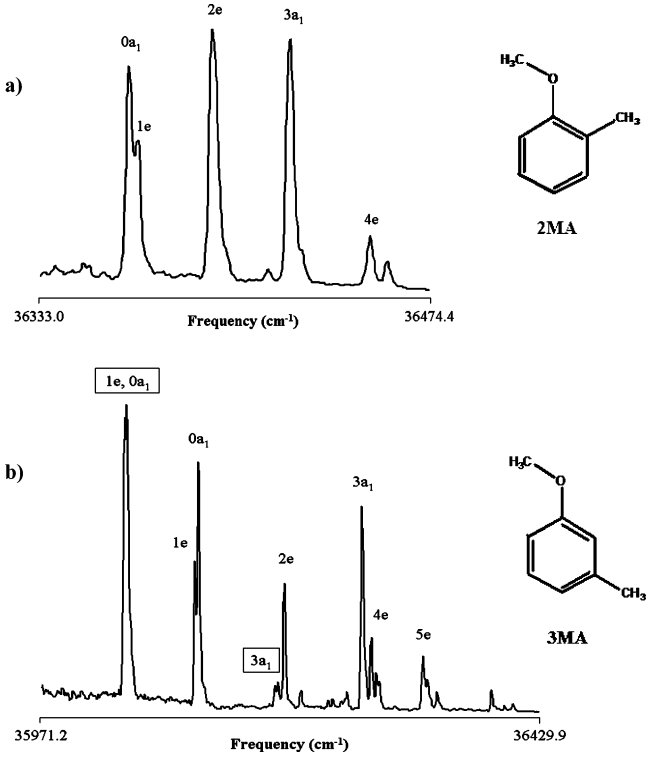

Figure 1. Vibrationally resolved fluorescence excitation spectra of 2MA (top) and 3MA (bottom) in the gas phase. The "boxed" labels refer to bands of the *cis*-conformer.

The expansion was skimmed 2 cm downstream with a 1 mm diameter skimmer and crossed 13 cm further downstream by a continuous wave (cw) Ar^+ pumped ring dye laser. The cw laser was operated with Rhodamine 110 dye and intracavity frequency doubled in BBO, yielding ~200 μW of UV radiation with a linewidth of ~1 MHz.

The fluorescence excitation spectrum was detected, using spatially selective optics, by a PMT and photon counting system. The PMT signal together with the iodine absorption spectrum and the relative frequency markers were simultaneously collected and processed by the jb95a data acquisition system.[12] Absolute frequency calibration of the spectra was performed by comparison with the I_2 absorption spectrum. The relative frequency markers were obtained from a stabilized etalon with a free spectral range of 299.7520 ± 0.0005 MHz.

3. Results

Figure 1 shows the vibrationally resolved fluorescence excitation (low resolution) spectra of 2MA and 3MA. Like Breen et al.[6] and Ichimura and Suzuki (IS),[7] we observe extensive low frequency progressions in each spectrum. (Additional activity appears at high energies in both spectra, in combination with ring modes (e.g., $6b^1$, $6a^1$, and 1^1).) The labeling scheme in Figure 1 is taken directly from IS[7] in which the numbers designate the vibrational quantum numbers of the methyl group torsional levels in the S_1 state and the letters designate their symmetries. The origin band ($0a_1$) in 2MA is at 36361.8 cm^{-1} (~275 nm), red shifted from that of toluene[4] by more than 1000 cm^{-1}. IS[7] claim that 3MA exhibits two origin bands, one at 36049.3 cm^{-1} that has been assigned as the *cis*-conformer (the lowest frequency band in Figure 1b, marked "1e,$0a_1$" inside the box) and a slightly higher energy band at 36115.5 cm^{-1} that has been assigned as the *trans*-conformer (marked "$0a_1$" in Figure 1b); see below. Clearly, the extensive Franck−Condon progressions in these two spectra signal large differences in both the orientations of the methyl groups and the barriers opposing their motions in the two electronic states, if these interpretations are correct.

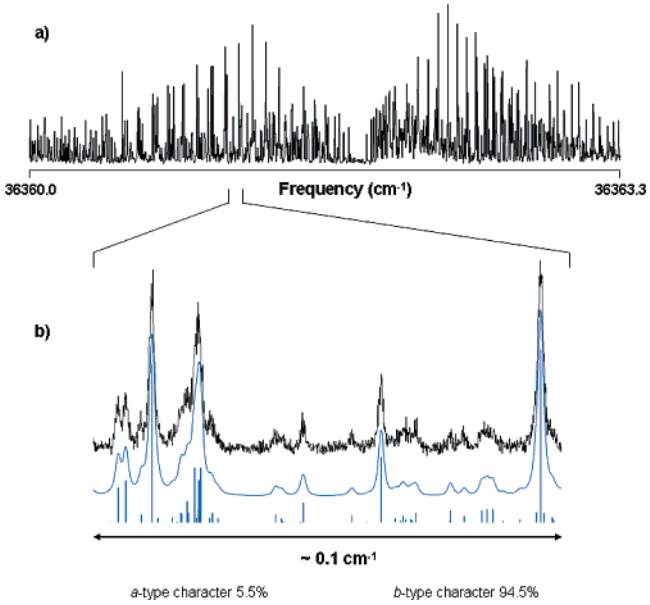

Figure 2. Rotationally resolved fluorescence excitation spectrum of band $0a_1$ in 2MA; the origin frequency is at 36361.8 cm^{-1}. A portion of the high resolution spectrum at full experimental resolution and its simulated spectrum are also shown in the bottom panel.

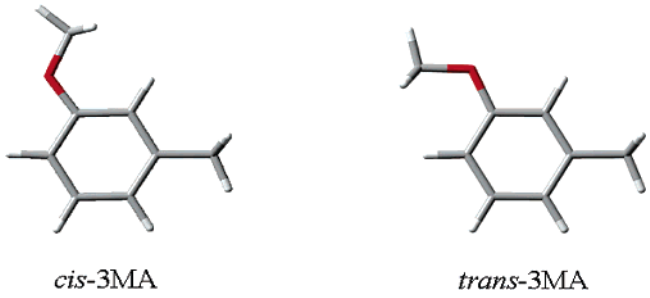

We have performed extensive studies of these spectra at high resolution, to test these hypotheses and to provide further information about the ensuing dynamics. Figure 2a shows the rotationally resolved $S_1 \leftarrow S_0$ fluorescence excitation spectrum of band $0a_1$ in 2MA. It spans approximately 3.3 cm^{-1} and exhibits *b*-type character, evidencing a near-perpendicular orientation of the $S_1 \leftarrow S_0$ transition moment in the inertial frame. To fit this spectrum, we first generated about ~2600 *b*-type rovibronic transitions based on *ab initio*[13] estimates of rotational constants and rigid rotor Hamiltonians for both electronic states. Then, we made quantum number assignments of single transitions in the simulated spectrum to corresponding transitions in the experimental spectrum, using the Windows-based program jb95.[14] Finally, we used a least-squares fitting procedure to optimize the rotational constants, based on a comparison of observed and calculated line positions. The final fit utilized 114 rovibronic transitions, including some weaker *a*-type lines and resulted in a standard deviation of 2.8 MHz. A portion of this fit is shown in Figure 2b. Individual lines in the fit exhibit Voigt profiles, with Gaussian widths of 18 MHz and Lorentzian widths of 28 MHz. The rotational temperature of the fit is 4 ± 1 K. The inertial parameters from the fit are reported in Table 1.

Band 1e was recorded but could not be analyzed. Other higher torsional bands, shown in Figure 1a, were analyzed, such as

TABLE 1: Rotational Constants of *trans*-2-Methylanisole in Its Ground and Excited Electronic States[a]

Parameter	2MA-0a_1	2MA-2e[b]	2MA-3a_1[c]
A'' (MHz)	2490.0 (1)	2490.6 (1)	2490.1 (1)
B'' (MHz)	1558.9 (1)	1558.8 (1)	1558.9 (1)
C'' (MHz)	970.7 (1)	970.7 (1)	970.7 (1)
A' (MHz)	2407.9 (1)	2419.2 (1)	2543.5 (1)
B' (MHz)	1550.0 (1)	1569.7 (1)	1830.9 (1)
C' (MHz)	951.2 (1)	952.3 (1)	954.1 (1)
$\Delta I''$ (amu Å^2)	−6.51 (2)	−6.52 (2)	−6.50 (2)
$\Delta I'$ (amu Å^2)	−4.64 (2)	−0.14 (2)	54.98 (3)
TM angle to the *b*-inertial axis	14 (2)°	14 (2)°	25 (2)°

[a] Numbers in parentheses are the standard deviations of the last significant figure. [b] See Table 5 for additional information about the first-order torsion−rotation perturbation coefficients that were used in the fit. [c] The following *A*-reduced Watson centrifugal distortion terms were applied to the S_1 state: $\Delta_J' = -0.10$, $\Delta_{JK}' = 0.15$, $\Delta_K' = -0.14$, $\delta_J' = 0.05$, $\delta_K' = 0.33$ MHz.

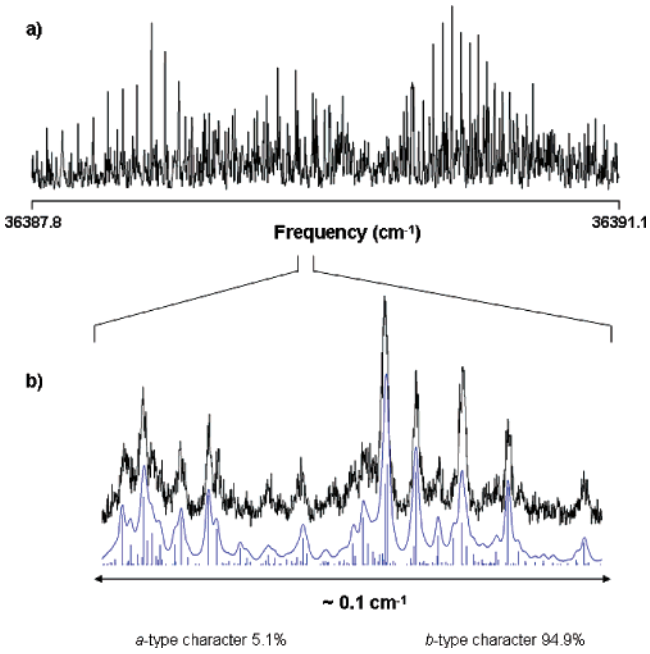

Figure 3. Rotationally resolved fluorescence excitation spectrum of band 2e in 2MA; the origin frequency is at 36389.7 cm^{-1}. A portion of the P-branch is also shown in the bottom panel.

bands 2e and 3a_1 in 2MA. Figure 3a shows the high resolution spectrum of 2MA-2e. Comparison of this spectrum with that in Figure 2a shows that band 2MA-2e has a very different structure. It appears to consist of two overlapping subbands, as would be expected if band 2MA-2e were in fact an "e-type" transition and the two subbands contained therein (e_1 and e_2) were split by the torsion−rotation interaction.[15] We therefore attempted to fit the spectrum in Figure 3a using the following Hamiltonian for both electronic states

$$H_{\text{eff}}^{E} = A_E P_a^{\,2} + B_E P_b^{\,2} + C P_c^{\,2} + F W_E^{(1)}(\rho_a P_a + \rho_b P_b) \quad (1)$$

Here, A_E, and so forth, are the effective rotational constants given by

$$A_E = A + F W_E^{(2)} \rho_a^{\,2}, \quad B_E = B + F W_E^{(2)} \rho_b^{\,2} \quad (2)$$

F is the internal rotor constant, $W_E^{(1)}$ and $W_E^{(2)}$ are the first- and second-order perturbation terms, first written down by Herschbach,[16] and ρ_a and ρ_b are weighted direction cosines of the angle between the axis of internal rotation and the *a*- and

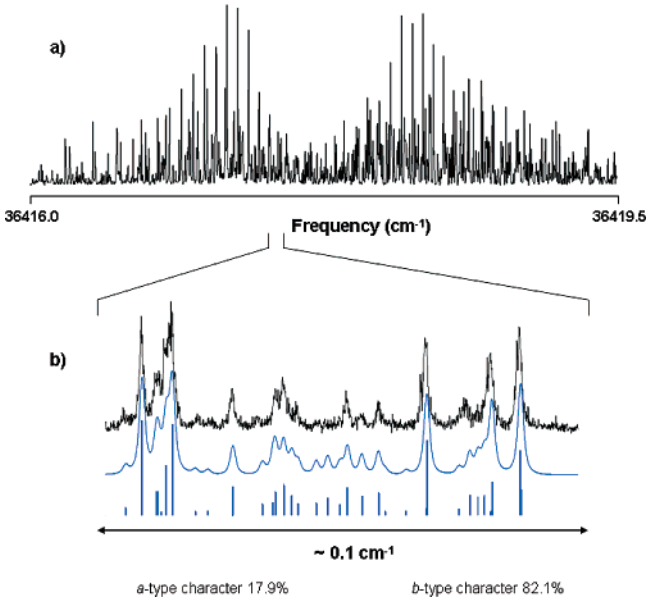

Figure 4. Rotationally resolved fluorescence excitation spectrum of band 3a_1 in 2MA; the origin frequency is at 36417.7 cm^{-1}. A portion of the high resolution spectrum at full experimental resolution and its simulated spectrum are also shown in the bottom panel.

b-inertial axes of the molecule, $\rho_a = \lambda_a(I_\alpha/I_a)$, and so forth. I_α is the moment of inertia of the methyl group, and r is a reduction factor

$$r = 1 - \sum (\lambda_g^{\,2} I_\alpha / I_g), \quad g = a,b,c \quad (3)$$

This fit showed excellent agreement with experiment, the OMC obtained was 3.8 MHz; see Figure 3b. The Gaussian line width in 2MA-2e is 18 MHz, the Lorentzian line width is 28 MHz, and the rotational temperature is 6 K. The inertial parameters obtained from this fit are listed in Table 1.

Figure 4a shows the high resolution spectrum of 2MA-3a_1. The fitting procedure for its analysis was analogous to that used for the 2MA-0a_1 band. Through the use of rigid-rotor Hamiltonians for both electronic states, a simulated spectrum was generated and more than 200 rovibronic simulated lines were assigned to experimental transitions, yielding an OMC of ∼20 MHz. This was reduced substantially to 3.9 MHz by including Watson distortion terms[17] for the S_1 state. The 3a_1 level lies above the torsional barrier in the S_1 state, but no torsion−rotation perturbations were observed which is consistent with the assignment of band 2MA-3a_1 as an a_1 band. This band has a Gaussian line width of 18 MHz, a Lorentzian line width of 30 MHz, and a rotational temperature of 4.5 K. Table 1 lists the inertial parameters obtained from the experimental fit of this band.

Figure 5a shows the high resolution spectrum of the lowest energy observed bands in 3MA, the "boxed" 3MA-1e,0a_1 band in Figure 1b. It spans approximately 6.6 cm^{-1} and displays two spectra on top of each other, as illustrated in Figure 5b. The blue-shifted spectrum was fit using effective rigid-rotor Hamiltonians for both states, which argues in favor of its assignment as the 0a_1 transition. However, the red-shifted band required first-order perturbation terms for its analysis, which argues in favor of its assignment as the 1e transition. Figure 5c shows a portion of the high resolution spectrum at full experimental resolution at the overlap region to illustrate the quality of the fit. The OMC of the fits are 2.4 MHz for the 0a_1 band and 3.1 MHz for the 1e band. The Gaussian line width is 18 MHz and the Lorentzian line width is 22 MHz for both bands. The inertial parameters for both spectra are reported in Table 2.

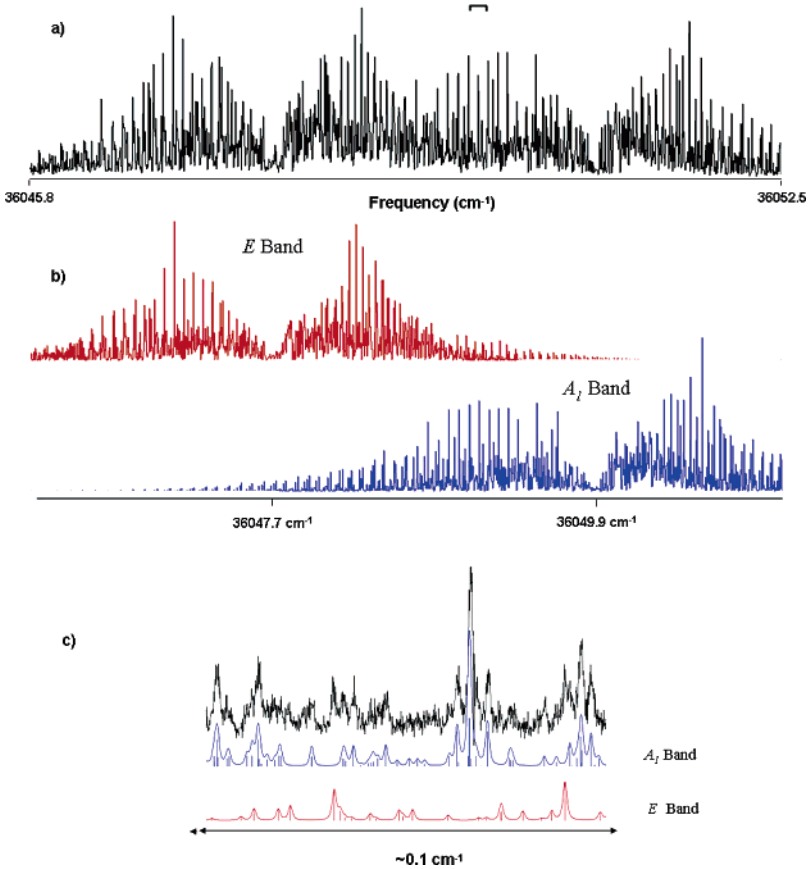

Figure 5. (a) Rotationally resolved fluorescence excitation spectrum of the *cis*-3MA-1e,0a_1 band. (b) Two simulated spectra (A_1 and E bands) are required to fit the experimental spectrum; the origin frequencies of each simulated spectrum are labeled on the horizontal axis. (c) A portion (see part a) of the fully resolved experimental spectrum and the detailed contribution of A_1- and E-type simulated rovibronic lines.

TABLE 2: Rotational Constants of *cis*-3-Methylanisole in Its Ground and Excited Electronic States[a]

Parameter	3MA-1e[b]	3MA-0a_1
A'' (MHz)	2752.0 (1)	2766.7 (1)
B'' (MHz)	1292.5 (1)	1297.5 (1)
C'' (MHz)	890.7 (1)	890.7 (1)
A' (MHz)	2676.4 (2)	2677.4 (1)
B' (MHz)	1279.2 (2)	1279.6 (1)
C' (MHz)	875.7 (1)	875.8 (1)
$\Delta I''$ (amu Å^2)	−7.22 (2)	−4.76 (4)
$\Delta I'$ (amu Å^2)	−6.79 (2)	−6.64 (4)
TM angle to the *b*-inertial axis	28 (2)°	25 (2)°

[a] Numbers in parentheses are the standard deviations of the last significant figure. [b] See Table 5 for additional information about the first-order torsion−rotation perturbation coefficients that were used in the fit.

Figure 6a shows the high resolution spectrum of the band labeled 3MA-0a_1 in Figure 1b. This spectrum spans ∼3.7 cm^{-1}, and its origin is located at 36115.5 cm^{-1}. Rigid-rotor Hamiltonians were found to be adequate to fully analyze this band; neither distortion terms nor perturbation coefficients were required. This confirms its assignment as an a_1 band. In the final fit, approximately 176 rovibronic lines were assigned and resulted in a standard deviation of 3.1 MHz. The Gaussian line width is 18 MHz, the Lorentzian line width is 20 MHz, and the rotational temperature is 5 K. The inertial parameters from the fit are listed in Table 3.

The 3MA bands labeled "1e" and "2e" in Figure 1b were both observed in our high resolution experiments, located at 36111.6 and 36193.6 cm^{-1}, respectively. Both bands were confirmed to be "e-type" bands as each is split by torsion−rotation coupling. Unfortunately, we have not yet succeeded in completely analyzing either of these bands; they are significantly perturbed and exhibit low signal-to-noise. Nonetheless, we can confirm that the origin of the 1e band is red shifted by 3.9 cm^{-1} from 0a_1 and that 2e is blue shifted by 82.0 cm^{-1} from 3a_1, as observed by IS.[7]

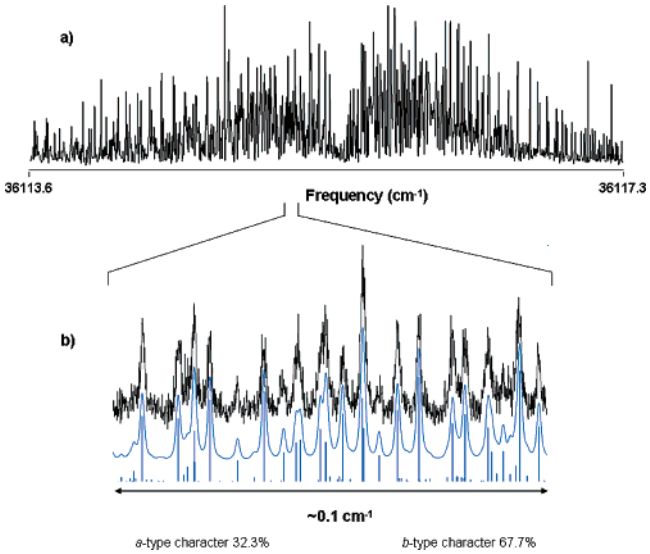

Figure 6. Rotationally resolved fluorescence excitation spectrum of the *trans*-3MA-0a_1 band; the origin frequency is at 36115.5 cm^{-1}. A portion of the high resolution spectrum at full experimental resolution and its simulated spectrum are also shown at the bottom panel.

Finally, Figure 7a shows the high resolution spectrum of 3MA-3a_1, located at 36264.3 cm^{-1}. It spans ∼4.7 cm^{-1} and has a congested Q-branch. Effective rigid-rotor Hamiltonians

TABLE 3: Rotational Constants of *trans*-3-Methylanisole in Its Ground and Excited Electronic States[a]

Parameter	3MA-$0a_1$	3MA-$3a_1$
A'' (MHz)	3573.1 (1)	3572.4 (1)
B'' (MHz)	1124.2 (1)	1124.1 (1)
C'' (MHz)	861.1 (1)	861.1 (1)
A' (MHz)	3406.5 (1)	3554.4 (2)
B' (MHz)	1111.3 (1)	1114.2 (2)
C' (MHz)	847.2 (1)	846.5 (1)
$\Delta I''$ (amu Å^2)	−4.06 (2)	−4.13 (1)
$\Delta I'$ (amu Å^2)	−6.62 (2)	1.26 (1)
TM angle to the *b*-inertial axis	34 (2)°	35 (2)°

[a] Numbers in parentheses are the standard deviations of the last significant figure.

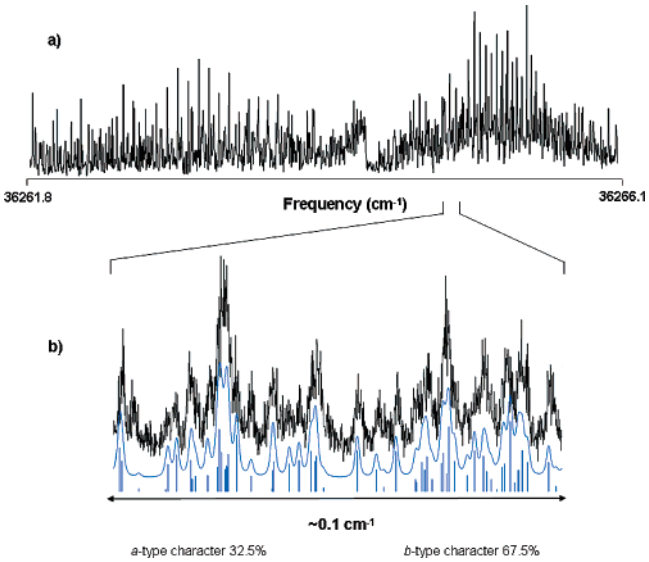

Figure 7. Rotationally resolved fluorescence excitation spectrum of the *trans*-3MA-$3a_1$ band; the origin frequency is at 36264.3 cm^{-1}. A portion of the high resolution spectrum at full experimental resolution and its simulated spectrum are also shown in the bottom panel.

were used to fit this band; no Watson distortion terms or first-order perturbation terms were required in the Hamiltonians to fit the spectrum. In the final fit, the convoluted spectrum showed mainly *b*-type rovibronic transitions but included some weaker *a*-type lines. Approximately 250 transitions were assigned and resulted in a standard deviation of 4.0 MHz. Figure 7b shows a portion of the R-branch at full experimental resolution to illustrate the quality of the fit. The Gaussian line width is 18 MHz, the Lorentzian line width is 20 MHz, and the rotational temperature is 8 K. Table 3 lists the inertial parameters obtained from the fit of this higher torsional band.

4. Discussion

4.1. Ground State Conformers. Table 4 compares the ground state rotational constants of the origin ($0a_1 \leftarrow 0a_1$) bands

TABLE 4: Experimental and Theoretical Ground State Rotational Constants from the Fits of the Origin Bands ($0a_1 \leftarrow 0a_1$) of *trans*-2MA, *cis*-3MA, and *trans*-3MA

Rotational constant	*trans*-2MA		*cis*-2MA	*cis*-3MA		*trans*-3MA	
	fit	theory[a]	theory[b]	fit	theory[a]	fit	theory[a]
A'' (MHz)	2490.0	2494.1	3333.3	2766.7	2752.1	3573.1	3532.3
B'' (MHz)	1558.9	1556.8	1461.7	1297.5	1295.2	1124.2	1121.8
C'' (MHz)	970.7	970.2	1029.2	890.7	890.5	861.1	860.6

[a] Geometry optimization calculation (MP2/6-31G**). [b] Single-point calculation (MP2/6-31G*).

obtained from our fits with the corresponding theoretical values for the *cis*- and *trans*-conformers of 2MA and 3MA. The data clearly show that the *cis*-2MA conformer was not present in our experiments. Therefore, we assign all the spectral features in Figure 1a to the *trans*-2MA conformer. On the other hand, both *cis* and *trans*-conformers were present in our experiments on 3MA; we assign the "boxed" 3MA-1e,$0a_1$ band in Figure 1b to the *cis*-3MA conformer, whereas the bands 3MA-$0a_1$ and 3MA-$3a_1$ are assigned to the *trans*-3MA conformer.

Differences among the ground state rotational constants may be easily understood. Figure 8 shows projections of the three geometry optimized[13] conformer structures in the *ab* plane, in their ground states. In *trans*-2MA, the A'' rotational constant is the smallest of the three because the methyl group is maximally displaced from the *a*-inertial axis, whereas the A'' rotational constant of the *trans*-3MA conformer is the largest among the three species because most of its heavy atoms lie close to the *a*-axis. *cis*-3MA is intermediate in this regard. The B'' and C'' rotational constants are similarly unique; *trans*-2MA has the largest B'' and C'' values, whereas *trans*-3MA has the smallest B'' and C'' values. The inertial defect values ($\Delta I = I_c - I_a - I_b$) of each conformer are expected to be near −6.6 amu Å^2; 2MA and 3MA should be planar structures in their S_0 state, with four out-of-plane hydrogen atoms, two from the methyl group and two from the methoxy group. However, the experimental values (see Tables 1, 2, and 3) are different; *trans*-2MA has $\Delta I'' = -6.51$ amu Å^2, but *cis*-3MA has $\Delta I'' = -4.76$ and *trans*-3MA has $\Delta I'' = -4.06$ amu Å^2. As will be seen, these deviations from experiment signal large motion along the methyl group torsional coordinate.

4.2. Excited State Conformers. Also shown in Figure 8 are the experimentally determined orientations of the $S_1 \leftarrow S_0$ transition moment (TM) vectors in the inertial frames of the three observed conformers of 2MA and 3MA. Immediately apparent is the fact that the observed TM vectors are approximately perpendicular to the C−O bond of the attached methoxy group, in all three cases. (Small differences in these orientation angles presumably have their origins in small rotations of the in-plane inertial axes by the attached methyl groups.) We conclude from this observation that the $S_1 \leftarrow S_0$

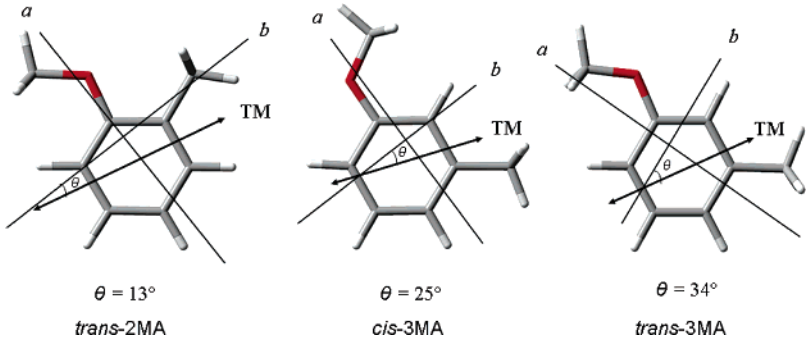

Figure 8. Inertial axes and $S_1 \leftarrow S_0$ TM orientation vectors in the experimentally observed *cis*- and *trans*-conformers of 2MA and 3MA.

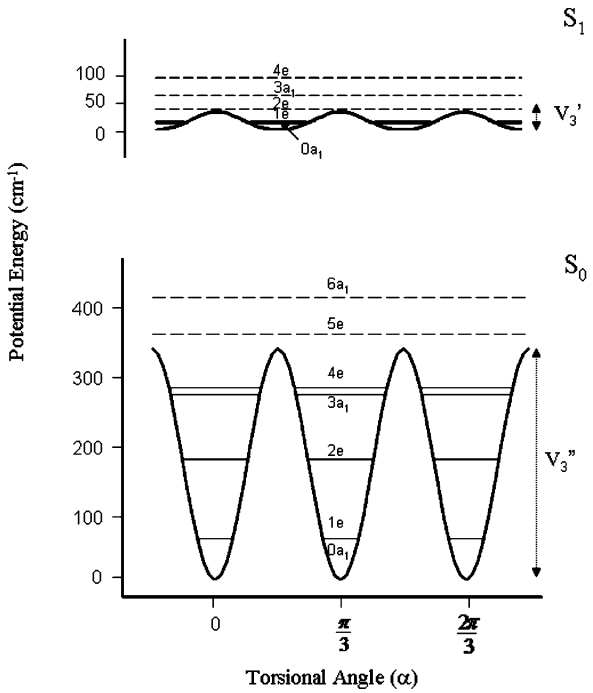

Parameter	Value (cm^{-1})
V_3	-36.90
V_6	-2.76
F	5.43

Parameter	Value (cm^{-1})
V_3	345.00
V_6	-5.00
F	5.50

Figure 9. Torsional energy surfaces of *trans*-2MA. The torsional parameters from the fit are included in tables for both electronic states.

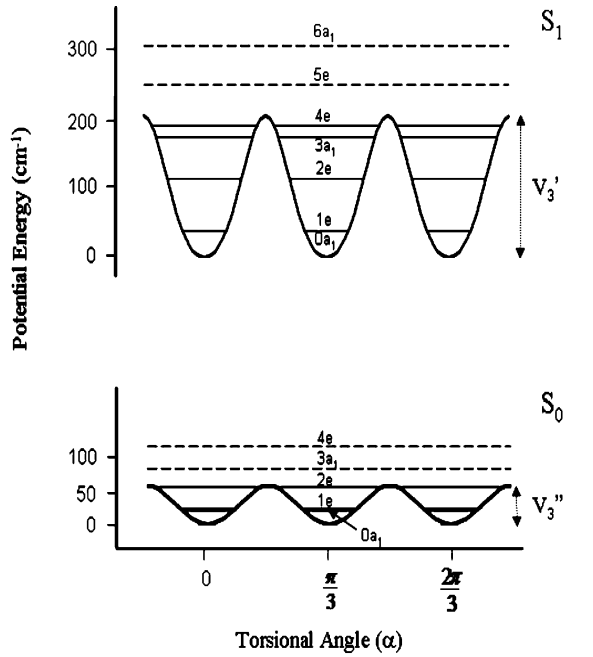

Parameter	Value (cm^{-1})
V_3	209.47
V_6	-26.00
F	5.51

Parameter	Value (cm^{-1})
V_3	57.07
V_6	2.00
F	5.46

Figure 10. Torsional energy surfaces for *cis*-3MA. The torsional parameters from the fit are included in tables for both electronic states.

transition in both 2MA and 3MA is "anisole-like"; that is, the $S_1 \leftarrow S_0$ transitions in all three conformers are principally HOMO−LUMO in nature and the nodal planes of these MOs are either parallel or perpendicular to the C−O bond. This has been confirmed by CIS calculations.[13]

The S_1 state of anisole is quinoidal in shape, expanded relative to the ground state, but with shorter "parallel" C−C bonds than perpendicular ones.[5,18,19] Thus, the three rotational constants A', B', and C' are all less than those of the ground state, but $\Delta A = (A' - A'') = -233$ MHz is by far the largest in magnitude. The same is true for all three observed conformers of 2MA and 3MA; *trans*-3MA has by far the largest value, $\Delta A = -167$ MHz. So, just as in anisole itself, there is significant charge transfer from the oxygen lone pairs of the methoxy group to the aromatic ring when both 2MA and 3MA absorb light.

4.3. Methyl Torsional Barriers. Despite the transfer of electrons from the oxygen atom to the ring, there is little or no torsional activity in the $S_1 \leftarrow S_0$ spectrum of anisole, presumably because of hyperconjugative interactions of the (methoxy) methyl group and the "in-plane" oxygen lone pair electrons. Charge transfer is expected to involve the "out-of-plane" oxygen lone pair. Thus, assuming the same to be true in 2MA and 3MA, the low frequency activity in their $S_1 \leftarrow S_0$ spectra must have its origin in the motion of the attached methyl groups. We focus on this issue here.

Table 5 lists the torsional parameters D_g ($= FW_E^{(1)}\rho_g P_g$, $g = a,b,c$), obtained from the fits of the 2e band in *trans*-2MA and the 1e band in *cis*-3MA. By the use of Herschbach's tables,[16] the reduced barriers (s) and the corresponding 3-fold barriers V_3 ($= {}^9/_4 F \cdot s$) were determined. Small torsion−rotation terms

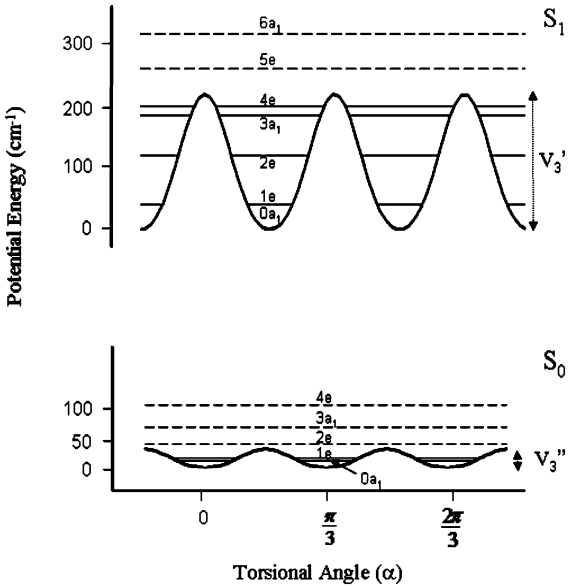

Parameter	Value (cm^{-1})
V_3	-225.70
V_6	-24.45
F	5.51

Parameter	Value (cm^{-1})
V_3	30.35
V_6	2.00
F	5.47

Figure 11. Torsional energy surfaces of *trans*-3MA. The torsional parameters from the fit are included in tables for both electronic states.

TABLE 5: First-order Torsion−rotation Perturbation Coefficients in the Hamiltonian and Reduced Barrier Heights for Selected *e*-Symmetry Torsional Bands in 2MA and 3MA[a]

Parameter	*trans*-2MA-2e band	*cis*-3MA-1e band
	Ground State (S_0)	
D_a'' (MHz)	4.6 (16)	1119.5 (3)
D_b'' (MHz)	16.3 (24)	667.4 (1)
$W^{(1)''}$	0.008	0.647
s''	27.879	4.685
V_3'' (cm^{-1})	345.00	57.07
V_6'' (cm^{-1})	−5.00	2.00
F'' (cm^{-1})	5.50	5.46
	Excited State (S_1)	
D_a' (MHz)	−2120.0 (1)	61.9 (3)
D_b' (MHz)	−3970.2 (1)	44.8 (30)
$W^{(1)'}$	2.531	0.038
s'	3.020	17.195
V_3' (cm^{-1})	−36.90	209.47
V_6' (cm^{-1})	−2.76	−26.00
F' (cm^{-1})	5.43	5.51

[a] Numbers in parentheses are the standard deviations of the last significant figure.

were found for *trans*-2MA ($D_a'' = 4.6$ and $D_b'' = 16.3$ MHz) in its S_0 state, which results in a relatively small first-order perturbation coefficient ($W_E^{(1)} = 0.008$), and by interpolation, a relatively large reduced barrier height of 27.879 ($V_3'' = 345.00$ cm^{-1}). A similar procedure was followed for the S_1 state, obtaining the much smaller barrier height of $V_3' = -36.90$ cm^{-1}, a value 10 times smaller than that computed for V_3''. Interestingly, *cis*-3MA exhibits the opposite behavior; its torsion−rotation terms are large in the ground state but small in the excited state, resulting in barriers of $V_3'' = 57.07$ cm^{-1} and V_3' = 209.47 cm^{-1}. The latter result perfectly agrees with the observation that the 1e transition in *cis*-3MA is red shifted from the $0a_1$ one. For the *trans*-3MA conformer, a different approach was used to determine the methyl torsional barriers. In this case, we performed an absolute frequency (energy) study to match the energy level spacings observed in our high resolution spectra. From those differences, the V_3, V_6, and F parameters were fit, $V_3'' = 30.35$ cm^{-1} and $V_3' = -225.70$ cm^{-1}. The corresponding potential energy surfaces for the three conformers studied are shown in Figures 9−11. The results for the *trans*-2MA and *trans*-3MA conformers are in close agreement with the ones obtained by IS.[7]

The significant differences in the ground state barriers, the excited state barriers, and the preferred orientation of the methyl groups among the three conformers have their origin in the relative positions of the substituents (S) attached to the aromatic ring, see below.

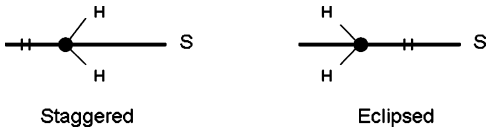

According to theory,[13] the eclipsed configuration of the methyl group is the more stable in S_0 *trans*-2MA, presumably due to the mesomeric effect. The C_1-C_2 bond is expected to have higher double bond character than C_2-C_3. However, excitation of 2MA to its S_1 state increases the π-character of the C_2-C_3 bond, owing to the quinoidal distribution of the ring. This explains both the dramatic reduction of V_3 on absorption of light and the conformational change of the methyl group, from the eclipsed to the staggered configuration. Apparently, the C_2-C_3 bond in *trans*-2MA has slightly more double bond character than the C_1-C_2 bond, in the S_1 state.[21,22]

The most stable configurations in ground state *cis*-3MA and *trans*-3MA are eclipsed and staggered, respectively; here, the relative orientation of the methoxy group determines which of the adjacent C−C ring bonds is strengthened by the mesomeric effect. Since *cis*-3MA has an eclipsed methyl group in its S_0 state, excitation of this state will only increase the magnitude of V_3 and not change its sign. No conformational change is observed. In contrast, *trans*-3MA has a staggered methyl group in its S_0 state, so that excitation by light changes both the barriers and its sign, resulting in a change of the preferred orientation of the methyl group.

The most remarkable consequences of these changes are the differences in relative intensities among the torsional bands and the Franck−Condon (FC) activity in the low frequency region of the vibrationally resolved spectra. *trans*-2MA shows FC activity, and its *A*/*E* intensity ratio[23] is about 2; the origin is not the most intense transition in the $S_1 \leftarrow S_0$ spectrum. On the other hand, *cis*-3MA exhibits a strong origin band, no FC activity, and an *A*/*E* intensity ratio of about 1; whereas *trans*-

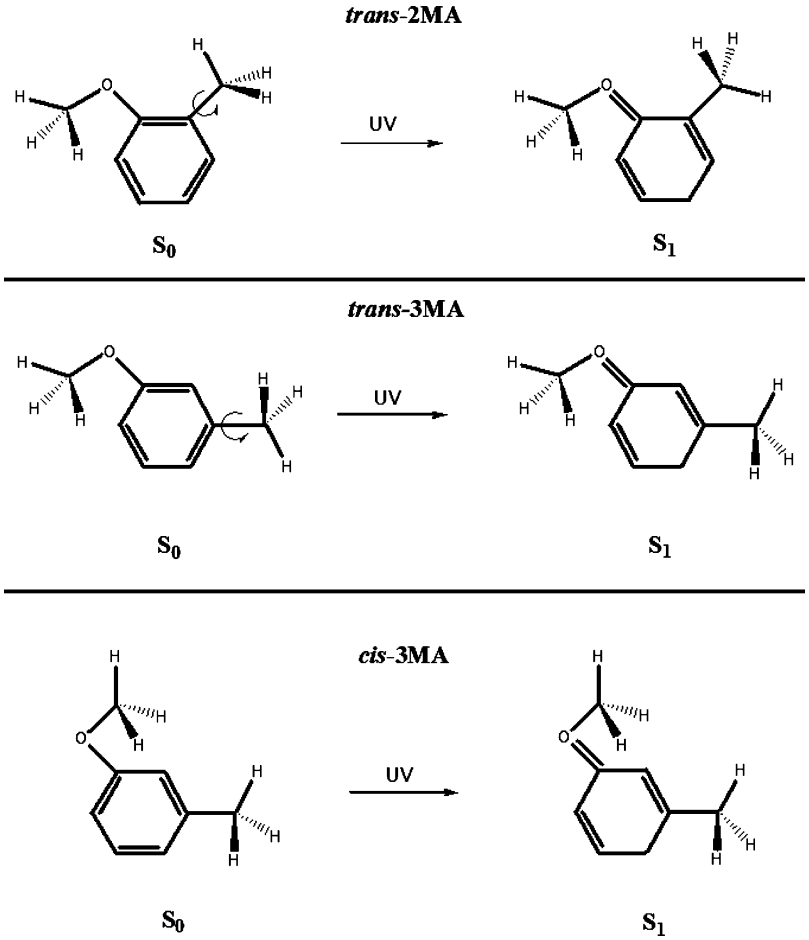

Figure 12. Most stable conformers of 2MA and 3MA in the gas phase.

3MA shows FC activity and an *A*/*E* intensity ratio near 2. These results are summarized in Figure 12.

A final, unanticipated result of these experiments is the discovery that the inertial defects of the three observed conformers of 2MA and 3MA are markedly influenced by the torsional motion of the methyl group. Recall from Table 1 that $\Delta I'' = -6.51$ amu Å^2 for *trans*-2MA in its ground state and $\Delta I' = -4.64$ amu Å^2 in the zero-point vibrational level of its excited electronic state. The larger (in magnitude) value is that expected for four out-of-plane hydrogen atoms, two from the methoxy group and two from the methyl group, whereas the smaller value is unexpected. In *cis*- and *trans*-3MA, this behavior is reversed; both molecules exhibit larger ΔI values in the excited state and smaller ΔI values in the ground state. The smaller values must signal transition to less "localized" methyl group C−H bonds, owing to the onset of essentially free internal rotation. Toluene, a molecule having a methyl group with similar properties, has ΔI values of −0.187 and 0.029 amu Å^2 in its S_0 and S_1 electronic states, respectively.[4] Still more surprising are the excited state ΔI values for the two higher energy vibronic bands in *trans*-2MA, −0.14 amu Å^2 for the 2e band and 54.98 amu Å^2 for the $3a_1$ band. The latter value may signal a large in-plane distortion of the isolated molecule.

5. Summary

Rotationally resolved $S_1 \leftarrow S_0$ fluorescence excitation spectra of three conformers of 2- and 3-methylanisole reveal that the position of substitution of the methoxy group on the aromatic ring determines the preferred orientation and torsional barrier height of the attached methyl group. The relative position of the two groups also has a major influence on the torsional dynamics. Comparisons of the results for the different electronic states show that these effects have their origin in substituent-induced differences in the π-electron distributions in the aromatic ring.

Acknowledgment. We thank Dr. David R. Borst, Dr. Cheolhwa Kang, and Dr. W. Leo Meerts for helpful assistance and suggestions. This work has been supported by NSF (CHE-0315584).

References and Notes

(1) (a) Kemp, J. D.; Pitzer, K. S. *J. Chem. Phys.* **1936**, *4*, 749. (b) Kemp, J. D.; Pitzer, K. S. *J. Am. Chem. Soc.* **1937**, *59*, 276.

(2) Pophristic, V.; Goodman, L. *Nature* **2001**, *411*, 565 and references therein.

(3) For a review, see Spangler, L. H.; Pratt, D. W. In *Jet Spectroscopy and Molecular Dynamics*; Hollas, J. M., Phillips, D., Eds.; Chapman & Hall: London, 1995; pp 366−398 and references therein.

(4) Borst, D. R.; Pratt D. W. *J. Chem. Phys.* **2000**, *113*, 3658.

(5) Ribblett, J. W.; Sinclair, W. E.; Borst, D. R.; Yi, J. T.; Pratt, D. W. *J. Phys. Chem. A.* **2006**, *110*, 1478.

(6) Breen, P. J.; Bernstein, E. R.; Secor, H. V.; Seeman, J. I. *J. Am. Chem. Soc.* **1989**, *111*, 1958.

(7) Ichimura, T.; Suzuki, T. *J. Photochem. Photobiol., C* **2000**, *1*, 79.

(8) Kojima, H.; Miyake, K.; Sakeda, K.; Suzuki, T.; Ichimura, T.; Tanaka, N.; Negishi, D.; Takayanagi, M.; Hanazaki, I. *J. Mol. Struct.* **2003**, *665*, 185.

(9) Kinoshita, S.; Kojima, H.; Suzuki, T.; Ichimura, T.; Yoshida, K.; Sakai, M.; Fujii, M. *Phys. Chem. Chem. Phys.* **2001**, *3*, 4889.

(10) Nakai, H.; Kawai, M. *J. Chem. Phys.* **2000**, *113*, 2168.

(11) Del Rio, A.; Boucekkine, A.; Meinnel, J. *J. Comput. Chem.* **2003**, *24*, 2093.

(12) Majewski, W. A.; Pfanstiel, J. F.; Plusquellic, D. F.; Pratt, D. W. In *Laser Techniques in Chemistry*; Rizzo, T. R., Myers, A. B., Eds.; J. Wiley & Sons: New York, 1995; p 101.

(13) Frisch, M. J.; Trucks, G. W.; Schlegel, H. B.; Scuseria, G. E.; Robb, M. A.; Cheeseman, J. R.; Montgomery, J. A., Jr.; Vreven, T.; Kudin, K. N.; Burant, J. C.; Millam, J. M.; Iyengar, S. S.; Tomasi, J.; Barone, V.; Mennucci, B.; Cossi, M.; Scalmani, G.; Rega, N.; Petersson, G. A.; Nakatsuji, H.; Hada, M.; Ehara, M.; Toyota, K.; Fukuda, R.; Hasegawa, J.; Ishida, M.; Nakajima, T.; Honda, Y.; Kitao, O.; Nakai, H.; Klene, M.; Li, X.; Knox, J. E.; Hratchian, H. P.; Cross, J. B.; Adamo, C.; Jaramillo, J.; Gomperts, R.; Stratmann, R. E.; Yazyev, O.; Austin, A. J.; Cammi, R.; Pomelli, C.; Ochterski, J. W.; Ayala, P. Y.; Morokuma, K.; Voth, G. A.; Salvador, P.; Dannenberg, J. J.; Zakrzewski, V. G.; Dapprich, S.; Daniels, A. D.; Strain, M. C.; Farkas, O.; Malick, D. K.; Rabuck, A. D.; Raghavachari, K.; Foresman, J. B.; Ortiz, J. V.; Cui, Q.; Baboul, A. G.; Clifford, S.; Cioslowski, J.; Stefanov, B. B.; Liu, G.; Liashenko, A.; Piskorz, P.; Komaromi, I.; Martin, R. L.; Fox, D. J.; Keith, T.; Al-Laham, M. A.; Peng, C. Y.; Nanayakkara, A.; Challacombe, M.; Gill, P. M. W.; Johnson, B.; Chen, W.; Wong, M. W.; Gonzalez, C.; Pople, J. A. *Gaussian 03*, revision A.1; Gaussian, Inc.: Pittsburgh, PA, 2003.

(14) Plusquellic, D. F. *Jb95 Spectral fitting program*; NIST: Gaithersburg, MD. http://physics.nist.gov/jb95.

(15) (a) Tan, X.-Q.; Majewski, W. A.; Plusquellic, D. F.; Pratt, D. W.; Meerts, W. L. *J. Chem. Phys.* **1989**, *90*, 2521. (b) Tan, X.-Q.; Majewski, W. A.; Plusquellic, D. F.; Pratt, D. W. *J. Chem. Phys.* **1991**, *94*, 7721.

(16) Herschbach, D. R. *J. Chem. Phys*. **1959**, *31*, 91.

(17) Watson, J. K. G. In *Vibrational Spectra and Structure*; Durig, J. R., Ed.; Elsevier: Amsterdam, The Netherlands, 1977; Vol. 6, p 1.

(18) Cvitas, T.; Hollas, J. M.; Kirby, G. H. *Mol. Phys*. **1970**, *19*, 305.

(19) Eisenhardt, C. G.; Pietraperzia, G.; Becucci, M. *Phys. Chem. Chem. Phys.* **2001**, *3*, 1407.

(20) Gordy, W.; Cook, R. L. *Microwave Molecular Spectra*; John Wiley & Sons: New York, 1984; p 570.

(21) That the barriers to internal rotation might be different in different electronic states was first proposed by Hehre, W. J.; Pople, J. A.; Devaquet, A. J. P. *J. Am. Chem. Soc*. **1976**, *98*, 664. See also ref 22.

(22) For a complete summary of methyl group barrier heights in aromatic molecules, see Zhao, Z.-Q.; Parmenter, C. S.; Moss, D. B.; Bradley, A. J.; Knight, A. E. W.; Owens, K. G. *J. Chem. Phys.* **1992**, *96*, 6362 and references therein.

(23) It has been described in ref 15b that the *A*/*E* intensity ratio varies from 1.0 to 3.0 when the phase factor changes from 0° to 60°, for V_3 values on the order of 100 cm^{-1}.